VAK 2024 MODERN ASTRONOMY: FROM THE EARLY UNIVERSE TO EXOPLANETS AND BLACK HOLES
300 years Russian Academy of Sciences

Current status of the Big Trio search program for distant radio galaxies. New radio data

O. Zhelenkova[1], Yu. Parijskij[2], N. Soboleva[2], and A. Temirova[2]

[1] Special Astrophysical Observatory of the Russian Academy of Sciences, Nizhny Arkhyz, 369167 Russia
[2] St. Petersburg Branch of the Special Astrophysical Observatory of the Russian Academy of Sciences, St. Petersburg, 196140 Russia

Abstract. The Big Trio programme was aimed to search for distant radio galaxies for the purpose of cosmological research. A selection of sources with steep and ultra-steep spectra was made from the radio sources discovered in a series of surveys by the Cold Experiment, which was carried out on the RATAN-600 radio telescope. The results of the studies of 113 sources in this sample were the optical identification of almost the entire sample, spectral studies of the majority of the objects (70%), spectral redshift determinations for half of them, and the discovery of three unique radio galaxies with redshifts $z > 3$ and extremely high radio luminosities. New radio sky surveys with high sensitivity and angular resolution have now become available, allowing additional studies of the radio sources in the sample. These have helped to refine the continuous spectra of the sources and their radiomorphology, as well as the evolutionary state and environment of the radio galaxies. The spectral indices determined from the new radio survey data turned out to be flatter than those from the old data. Based on the spectral curvature parameter and the morphological structure of the sources in the steep spectrum (SS) sample, 10–15% are likely to be young, 40–50% are in an active state, 10% are in the fading phase, and most likely 20–25% are in the restart phase.

Keywords: galaxies: active, high-redshift

DOI: 10.26119/VAK2024.042

1 Introduction

In the early 1990s, SAO RAS began work on the Big Trio programme (Goss et al. 1992; Parijskij et al. 2000), which aimed to search for distant radio galaxies and to study them further for cosmological purposes (Miley & De Breuck 2008). Three large telescopes were used for the observations: the RATAN-600 and VLA radio telescopes (NRAO, USA) and the 6-m BTA telescope. High angular resolution radio observations were made to refine the coordinates and determine the morphological structure of the sample of steep spectrum (SS) radio sources at the VLA. Photometric and spectral studies of the sample were performed on the 6-m BTA telescope. 94% of the radio sources were identified with their host objects, and spectra were obtained for 70% of the SS sample. Three unique radio galaxies with redshifts $z > 3$ and extremely high radio luminosities were discovered (Kopylov et al. 2006; Parijskij et al. 2010, 2014).

Thanks to the modern radio sky surveys TGSS (Intema et al. 2017), GLEAM (Hurley-Walker et al. 2017), RACS (McConnell et al. 2020), VCSS (Peters et al. 2021) and VLASS (Gordon et al. 2021) it was possible to once again refine the continuum spectra of the SS sample once again.

Access and analysis of the survey, catalog and tabular data was performed using the TOPCAT (Taylor 2005) and ALADIN (Bonnarel et al. 2000) software tools. The spg programme from the RATAN-600 (Verkhodanov et al. 1993) data processing system was used to construct the continuum spectra. The spectral index was determined from the spectra constructed by linear and parabolic approximations using weighting coefficients and discarding outliers. The spectral index of a radio source α is defined as $S_\nu \propto \nu^\alpha$.

2 Comparison of old and new continuum spectra

Initially, the selection of sources in the SS sample was made using a two-frequency spectral index $\alpha_{3940}^{365} \leq -0.9$ at 365 and 3940 MHz based on the integrated flux densities from the UTRAO and RC catalogs. In addition, double sources of small angular size were selected. In one of the early papers (Soboleva et al. 1994) 96% of the SS sample sources have a spectral index of ≤ -0.9. The spectra and spectral indices of the SS sample have been determined several times from measurements made with the RATAN-600 radio telescope and from data in publications mentioning the sources under study.

Here we compare the spectral indices of the SS sample sources obtained by fitting the spectra to three sets of integrated flux densities. One set is taken from Bursov et al. (1996). It covers the range 365–4850 MHz, and in some cases for bright sources

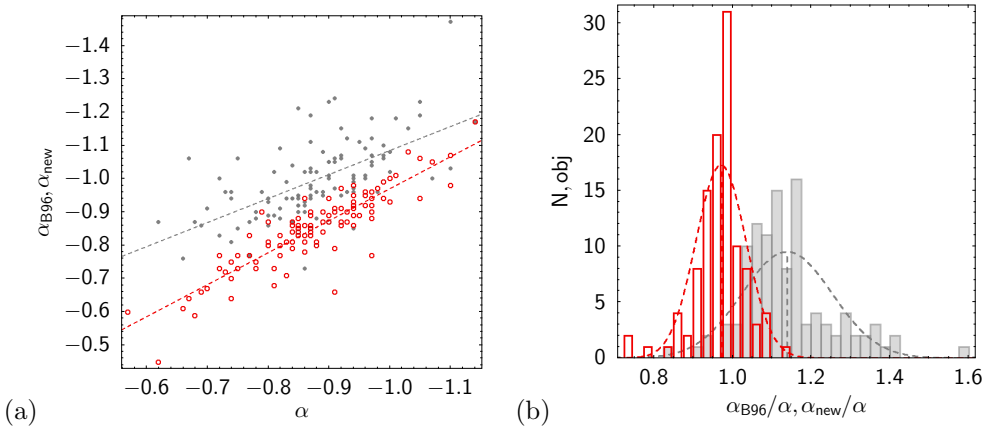

Fig. 1. The figure shows a scatterplot of the spectral indices (a). The spectral indices α_{B96} (grey dots) and α_{new} are plotted on the y-axis, and α on the x-axis. The dotted lines show the linear regression. The histogram (b) shows the distribution of the ratio of α_{B96} to α (grey) and the ratio of α_{new} to α (red). The dotted line shows the approximation of the distribution by the Gaussian function.

from 13 MHz to 11 GHz. The index α_{B96} is determined from this data. The second set contains data from the modern sky surveys VLSSr (Lane et al. 2014), TGSS, GLEAM, VCSS, RACS and VLASS. Flux densities for the sample sources are determined for up to 30 frequencies, mainly from 74 MHz to 3 GHz. The index α_{new} is calculated from these data. And the third data set, the most complete, contains the flux densities of the first two sets, i.e. all the information about the sources that is currently available. The index α is computed using this data set.

With the advent of the low-frequency TGSS and GLEAM surveys, we have been able to refine the spectral characteristics of some sources. For example, 19% of the objects have a curved spectrum of the type C^-. For 9% of the sources the spectrum type can be classified as C^+, which has been refined by adding new high-frequency data. Thus, 28% of the sources have a curved spectrum (C^- and C^+) or a spectrum with a single peak. Such types of spectra are better approximated by a parabola. The statistics of the spectral indices calculated from three sets of flux densities are given in Table 1. Since the linear approximation of curved spectra is at least reflects the spectral shape, the spectral indices will be erroneous. When comparing the spectra constructed by the linear approximation, we used a subsample of sources (72%) with straight spectra (S-type). The table also shows the median of the ratios of the first two spectral indices to the third spectral index, which we consider to be the most reliable. The table also shows the standard deviations for these ratios. This allows us to estimate the accuracy of the spectral indices.

Table 1. SS sample source statistics for three sets of flux densities: Set — the set of flux densities corresponding to the spectral index; $\alpha \leq -0.9$ — the percentage of sources in the SS sample that satisfy this condition; $\alpha_{\rm med}$ — the median value of the spectral index for the subsample of sources with $\alpha \leq -0.9$; $\alpha^{\rm SS}_{\rm med}$ – the median of the spectral index for the whole SS sample; Ratio – the ratio of the spectral index to α.

Set	$\alpha \leq -0.9$	$\alpha_{\rm median}$	$\alpha^{\rm SS}_{\rm median}$	Ratio
Linear fitting (S-type spectra)				
α_{B96}	89%	−1.01	−1.00	1.128±0.094
α_{new}	33%	−0.94	−0.86	0.973±0.040
α	46%	−0.96	−0.88	

Both Table 1 and Fig. 1 show some discrepancy between the spectral indices determined from the old and new data. It can be seen that the old spectral indices are steeper than the new ones.

3 Spectral cuvature and evolutionary state, morphology and environment

During their lifetime in the radio phase, AGNs go through the following stages: the birth of a radio source, its active phase, the fading of the radio source, when the AGN stops feeding jets, and a possible restart. To separate these phases, the spectral curvature parameter (SCP) is often used as the difference between the spectral indices of the high- and low-frequency regions of the spectrum (Murgia et al. 2011). The maximum curvature expected in the active phase is limited by SPC$\leq$0.5. On the other hand, the integral spectra of dying sources are characterised by an exponential cut-off at high frequencies, so that extreme spectral curvatures are possible for them (SCP$>$0.5). Finally, for restarting sources, the injection of new electrons flattens the high-frequency spectrum, resulting in SCP$<$0. This classification should be regarded as having statistical significance. For the SPC to be meaningful, it must be calculated over a frequency range of at least two orders of magnitude.

We calculated SCPs for the SS sample based on the spectra that were constructed using a parabolic fit to all currently available data. The spectral indices were calculated as $\alpha_{\rm low}$ and $\alpha_{\rm high}$ for 500 and 3940 MHz respectively. We also calculated the SCP in a different way. The $\alpha_{\rm low}$ were obtained from the GLEAM data by linear fitting of the spectra and the $\alpha_{\rm high}$ were obtained from the RACS, VCSS, and VLASS data. We found that the fading sources in the SS sample account for 8–10%, and the restarting sources account for 15–17%. Sources of small angular size with a peak in the spectrum (GPS and HFP) are thought to be young objects that later evolve into

FR-I and FR-II radio galaxies (Callingham et al. 2017). We have classified 10–15% of the sources as young.

The morphological structure of the source also carries information about evolutionary phases. The sources showing a double-double or triple structure (Brocksopp et al. 2011; Gopal-Krishna et al. 2012), are classified as AGN with radio phase restart. And we attributed 20–25% of the objects to this type of source. Comparing the NVSS and VLASS cutouts, we found that some sources have radio lobes at 1.4 GHz, but they are absent or weakly expressed in the 3 GHz maps. We classified such sources as fading (10%). And 40–50% of the radio sources in the sample are in the active phase.

The deformation of the lobes of the radio source is an indicator of its environment and/or the processes taking place in the immediate vicinity of the AGN. Tailed sources (Wide-Angle Tailed, Narrow-Angle Tailed, Head-Tailed) indicate that they may be located in clusters or groups of galaxies (Owen & Rudnick 1976; Missaglia et al. 2019). And there are 30% of such sources in the sample. The X-, Z-, S-shaped morphology of the radio lobes is explained by a rapid change in the orientation of the jets, either due to the merger of a small galaxy with a massive elliptical host galaxy, or due to instabilities in the accretion disk (Liu 2004; Joshi et al. 2019). In the sample, 14% of the radio sources have such a morphology.

4 Summary

By comparing the spectral indices obtained by linearly fitting the data from three sets of flux densities, we estimated the accuracy of the spectral indices for a subset of sources with C-type spectra. The error in the determination of the indices was 4–9%. The Figure 1 shows the discrepancy between the spectral indices determined from old and new data. It can be seen that the old spectral indices are steeper than the new ones. The number of sources satisfying the selection condition — spectral index less than or equal to -0.9 according to the new data has almost doubled. This may be due to the appearance of low-frequency data, in particular from the GLEAM survey, which allow continuum spectra to be more accurately determined.

Based on the shape of the deformed radio lobes, 30% of the sample sources are likely to be in a group or cluster of galaxies, and 14% show jet reorientation.

After calculating SCPs for the SS sample using spectral indices at 500 and 3940 MHz, we found that the sample contains 8–10% fading sources, 15–17% in the restart phase, and 10–15% young sources. The analysis of the morphological structure of the radio sources showed that 10% of the sources are fading and 20–25% are restarting. Thus, the SS sample contains radio sources with different evolutionary phases.

Acknowledgements. This research has made use of the VizieR catalogue access tool (Ochsenbein et al. 2000) and the SIMBAD database (Wenger et al. 2000), CDS, Strasbourg, France. The NASA/IPAC Extragalactic Database (NED), operated by the Jet Propulsion Laboratory, California Institute of Technology, on behalf of the National Aeronautics and Space Administration, was used in this search; the CATS database (Verkhodanov et al. 2005), available on the website of the Special Astrophysical Observatory.

References

Bonnarel F., Fernique P., Bienaymé O., et al., 2000, Astron. Astrophys., Suppl. Ser., 143, p. 33
Brocksopp C., Kaiser C. R., Schoenmakers, et al., 2011, Mon. Not. R. Astron. Soc., 410, p. 484
Bursov N.N., Lipovka N.M., Soboleva N.S., et al., 1996, Bulletin of the Special Astrophysics Observatory, 42, p. 5
Callingham J.R., Ekers R.D., Gaensler B.M., et al., 2017, Astrophys. J., 836, p. 174
Gopal-Krishna, Biermann P.L., Gergely L.´A., et al., 2012, Research in Astronomy and Astrophysics, 12, p. 127
Gordon Y.A., Boyce M.M., O'Dea C.P., et al., 2021, Astrophys. J., Suppl. Ser., 255, id. 30
Goss W.M., Pariiskii Y.N., Soboleva N.S., et al., 1992, Sov. Astron., 36, p. 343
Hurley-Walker N., Callingham J.R., Hancock P.J., et al., 2017, Mon. Not. R. Astron. Soc., 464, p. 1146
Intema H.T., Jagannathan P., Mooley K.P., et al., 2017, Astron. Astrophys., 598, id. A78
Joshi R., Krishna G., Yang X., et al., 2019, Astrophys. J., 887, p. 266
Kopylov A.I., Goss W.M., Parijskij Y.N., et al., 2006, Astronomy Letters, 32, p. 433
Lane W.M., Cotton W.D., van Velzen S., et al., 2014, Mon. Not. R. Astron. Soc., 440, p. 327
Liu F. K., 2004, Mon. Not. R. Astron. Soc., 347, p. 1357
McConnell D., Hale C.L., Lenc E., et al., 2020, Publ. Astron. Soc. Aust., 37, id. e048
Miley G. and De Breuck C., 2008, Astron. Astrophys., 15, p. 67
Missaglia V., Massaro F., Capetti A., et al., 2019, Astron. Astrophys., 626, id. A8
Murgia M., Parma P., Mack K. H., et al., 2011, Astron. Astrophys., 526, id. A148
Ochsenbein F., Bauer P., Marcout J., 2000, Astron. Astrophys., Suppl. Ser., 143, p. 23
Owen F.N. and Rudnick L., 1976, Astrophys. J., 205, id. L1
Parijskij Y.N., Goss W.M., Kopylov A.I., et al., 2000, Astronomical and Astrophysical Transactions, 19, p. 297
Parijskij Y.N., Kopylov A.I., Temirova A.V., et al., 2010, Astronomy Reports, 54, p. 675
Parijskij Y.N., Thomasson P., Kopylov A.I., et al., 2014, Mon. Not. R. Astron. Soc., 439, p. 2314
Peters W., Polisensky E., Brisken W., et al., 2021, American Astronomical Society Meeting Abstracts, 237, id. 211.06
Soboleva N.S., Pariiskii Y.N., Naugolnaya M.N., 1994, Astron. Zh., 71, p. 684
Taylor M.B., 2005, Astronomical Society of the Pacific Conference Series, 347, p. 29
Verkhodanov O.V., Erukhimov B.L., Monosov M.L., et al. 1993, Bulletin of the Special Astrophysics Observatory, 36, p. 132
Verkhodanov O.V., Trushkin S.A., Andernach H., et al., 2005, Bulletin of the Special Astrophysics Observatory, 58, p. 118
Wenger M., Ochsenbein F., Egret D., et al., 2000, Astron. Astrophys., Suppl. Ser., 143, p. 9